Synthesis of ZnO/PMMA nanocomposite by low-temperature atomic layer deposition for possible photocatalysis applications

Alessandro Di Mauro [a,*], Clayton Farrugia [b], Stephen Abela [b], Paul Refalo [c], Maurice Grech [b], Luciano Falqui [d], Vittorio Privitera [a], Giuliana Impellizzeri [a]

[a] CNR-IMM, Via S. Sofia 64, 95123, Catania, Italy
[b] Department of Metallurgy & Materials Engineering, Faculty of Engineering, University of Malta, Msida MSD, 2080, Malta
[c] Department of Industrial & Manufacturing Engineering, Faculty of Engineering, University of Malta, Msida MSD, 2080, Malta
[d] Plastica Alfa SpA, C. da Santa Maria Poggiarelli - Zona Industriale, Caltagirone (CT), Malta, 95041, Italy

ARTICLE INFO

ABSTRACT

Zinc oxide is one of the most widely used semiconductors, thanks to its shallow band-gap of 3.3 eV, low cost, inertness, and abundance in nature. On the other hand, poly (methyl methacrylate) (PMMA) is a common thermoplastic material used in many applications namely because of its transparency, environmental stability, and low cost. The realization of novel inorganic/polymeric hybrid nanomaterials is appealing, being beneficial in a variety of applications including photocatalysis, sensing, energy harvesting and storage, and optoelectronics, but also challenging. In this work, ZnO and PMMA were combined using the atomic layer deposition (ALD) technique. The morphology of the samples was evaluated by scanning electron microscopy (SEM), while the crystallinity has been investigated using X-ray diffraction (XRD) analyses. In order to give a proof of concept of a possible application of the materials synthetized, the photocatalytic activity of the nanocomposites has been tested by the degradation of two organic pollutants in water: methylene blue (MB) dye and sodium lauryl sulfate (SDS), an anionic surfactant. The results have shown that all samples are active in the removal of both pollutants (i.e., MB and SDS), opening the route for the application of the proposed nanocomposites in water treatment.

1. Introduction

Zinc oxide (ZnO) is a direct wide band-gap material ($\sim$ 3.4 eV at 300 K) with many advantages for opto-electronics, like the availability of large area substrates for epitaxial layer growth and high solubility of *n*-type dopants. These optical and crystallographic properties promote its use as a transparent conductive layer in transparent electronics and photovoltaics. A large exciton binding energy ($\sim$ 60 meV), and excellent luminescent properties gave rise to efficient light emitting devices operating in the blue/ultraviolet (UV) regime [1–4]. Furthermore, it has a high chemical/thermal stability and radiation hardness, it is non-toxic and eco-friendly, and is of low cost. Since being established as an electronic material in the 1950s, substantial progress has been made in the development of ZnO-based varistors, UV detectors, sensors, transducers, surface acoustic wave devices, and as a transparent and conductive oxide [1–4]. Given its high photocatalytic activity, zinc oxide has also received great attention as a photocatalytic semiconductor for environmental applications [5–8]. The interest was further motivated by the suitability of ZnO to form nanostructures, where a wide variety of shapes and sizes have been demonstrated [9–13].

The implementation of ZnO in real world applications is associated to its integration on a polymeric substrate or matrix. The latter would assure flexibility, formability, low weight, as well as low cost of manufacture. For this reason, the realization of hybrid materials, composed of an organic part (polymer-based) and an inorganic counterpart (ZnO-based), has recently attracted remarkable interest among the research community [14–20].

Zinc oxide is conventionally prepared by physical or chemical vapor deposition methods at substrate/reactor temperatures higher than 200 °C [21,22], temperatures which are incompatible with the thermally fragile polymers. Atomic layer deposition (ALD) presents itself as a viable deposition technique as it allows for the deposition of crystalline phases at close to room temperature. Over the conventional methods, ALD allows the production of materials with atomic scale precision together with a strict control of the structural and chemical properties on large areas [23,24]. The high quality of the ALD materials originates

---

from the peculiar growth mechanism based on selective and self-limiting reactions between the ALD gaseous precursors and the exposed reactive group at the surface of the substrate [23,24]. Compared with other deposition methods, ALD can operate at much milder conditions of pressure and temperature and in the absence of molecular-level bombardment, thus being compatible with the polymeric substrates. It is relevant to note that the deposition of ZnO on polymers using the ALD process is challenging. Firstly, it is necessary to work at a low deposition temperature, specifically below the glass transition temperature of the polymer to avoid the softening of the substrate and limit the dilatation of the polymer due to the phase change, which would introduce stresses in the film and cause delamination [23]. Secondly, polymers often lack the active surface sites necessary, in principle, for activating the film growth [23,25]. Finally, polymers may build a negative surface charge, which often repels the precursors and slows down the growth rate of the film produced by the ALD processes [26–29]. Some groups investigated the atomic layer deposition of ZnO on different polymers, such as poly-vinylidene fluoride [30], hydroquinone superlattice [31], poly-propylene [32], poly (methyl methacrylate) (PMMA) [33]. In case of polymer surfaces having no hydroxyl groups, the first precursor reaching the surface is trapped into the porous structure of the plastic mate-rial. Polymers like PMMA, polyvinyl chloride, polystyrene, polypropylene and others fall under this category. The trapped pre-cursors serve as nuclei on which the second precursor reaching them forms clusters and progressively grows and eventually coalesces, closing the space between the polymeric chains. Following that, the metal-oxide grows on the polymer's surface as a film [34]. This means that it is possible to produce thin films on polymers even in the absence of active surface sites. However, to achieve this process, the precursor has first to overcome the repulsive force generated by the accumulating surface charge that acts as a barrier [25,34].

PMMA substrates were chosen in this work as the organic component of the nanocomposites. This selection derived from the vast range of applications of PMMA, due to its transparency to visible light, its attractive mechanical properties, chemical stability, low-cost, and hy-drophobic characteristics when in contact with food and drinks. Although the ALD of ZnO on PMMA has been demonstrated [33,35,36], this method is still at an early stage, thus deserving further investigation.

In this work ZnO-PMMA based nanocomposites have been synthe-sized by ALD using mainly two different strategies: 1) the deposition of ZnO films by ALD on PMMA plates; 2) the coating of PMMA powders with a thin layer of ZnO by ALD and subsequent sonication and solution casting. A comparison with ZnO-PMMA materials simply synthetized through the sonication and solution casting method has been performed. The synthesized nanocomposites have been extensively characterized and tested for the degradation of organic pollutants in wastewater, as proof of a possible field of application of the proposed materials.

2. Experimental

2.1. Materials

Plates of PMMA (4 mm thick) synthetized by Plastica Alfa using in-jection molding, PMMA powders having a molecular weight of 120,000 Da and 0.2–1 mm in diameter purchased from Sigma Aldrich, and 8-inch (100)-oriented silicon wafers bought from Si-Mat, were employed as substrates for the ALD deposition processes. Diethyl zinc (DEZ) was purchased from Air Liquide and used as ALD precursors for the deposition of ZnO. Zinc acetate dihydrate (ZnAc$_2$·2H$_2$O), sodium hydroxide (NaOH), methylene blue (MB), and sodium lauryl sulfate (SDS) were purchased from Sigma-Aldrich and used as received.

2.2. Preparation

The ZnO-PMMA nanocomposites, presented in this paper, were synthesized using three different methods, described below.

Atomic layer deposition of ZnO on PMMA and Si plates: ZnO thin films were deposited on PMMA and Si substrates which measured 2.5 cm × 2.5 cm. The PMMA pieces were first washed in a solution of deionized water and isopropanol, and then dried under a nitrogen flux. The Si substrates were merely cleaned under a nitrogen flux. The de-positions of ZnO were performed using the ALD Picosun R-200 Advanced reactor. The deposition temperature was fixed at 80 °C, being lower than the softening temperature of the PMMA (glass transition temperature of PMMA is around 100 °C) [37]. Diethyl zinc (DEZ, purity 99.9999%) and deionized water were used as the precursors, while N$_2$ was used as the carrier and purge gas (purity ≥ 99.999%). The precursor temperatures were both set at 22 °C. The pulse and purge times were kept constant at 0.1/3.0/0.1/5.0 s for DEZ/N$_2$/H$_2$O/N$_2$. The number of ALD cycles was varied from 220 to 2200. These samples will be hereafter called: "ZnO ALD".

Atomic layer deposition of ZnO on PMMA powders and solution casting: PMMA powders were coated with a thin layer of ZnO using the ALD process. The deposition was performed using a POCA system [16], which is a powder coating solution consisting of a quartz glass with a porous separator on the bottom (pore size in the range of 160–250 μm). For this experiment, the POCA system was filled with 2 g of PMMA powders. The deposition of ZnO was performed as reported above for the deposition of ZnO on PMMA plates (i.e., 80 °C, 0.1/3/0.1/5 s for the DEZ/N$_2$/H$_2$O/N$_2$). Then, the ZnO-PMMA nanocomposites were pre-pared using the sonication and solution casting method [38,39]. 300 mg of ZnO-PMMA powders were dissolved in 5 mL of acetone. The solution was sonicated for about 8 h. After that, the mixture was cast into Petri dishes (5 cm in diameter) and dried overnight at 4 °C to favor the sedimentation of ZnO at the bottom of the films. The nanocomposite films were then peeled off from the Petri dishes. This material shall be referred to as: "ZnO ALD + Solution Casting".

ZnO-PMMA by sonication and solution casting: An easy fabrica-tion technique involves the mixing of a raw polymer with a semi-conductor, both in the powder form, in order to attain nanopowders embedded in a polymeric matrix [39]. ZnO nanopowders were firstly synthesized using a precipitation technique, as reported in literature [40]. During a typical synthesis, 20 mL of NaOH solution (1.0 M) and 20 mL of a ZnAc$_2$·2H$_2$O solution (0.5 M) were mixed in a flask and the solution was stirred for 2 h using a magnetic stirrer. The mixture was separated from water using a centrifuge rotated at 4000 rpm for 5 min. The powders collected were washed several times in distilled water and then dried overnight at 140 °C. Following this, the ZnO-PMMA com-posites were produced using the sonication and solution casting method [38,39]. Specifically, 800 mg of PMMA were dissolved in 4 mL of acetone, while 30 mg of ZnO nanopowders (synthesized as described before) were dispersed in 4 mL of acetone. Both the solution and the dispersion were sonicated for about 45 min. The inorganic dispersion was then added to the PMMA solution and mixed for 1 h. After that, the mixture was cast into Petri dishes (5 cm in diameter) and dried overnight at 4 °C to favor the sedimentation of ZnO at the bottom of the Petri dishes. The nanocomposite films were then peeled off from the Petri dishes. This material will be hereafter simply called: "ZnO Solution Casting".

2.3. Characterization

The thickness of the ZnO flat films was determined using the M − 2000 spectroscopic ellipsometer by Woollam, applying a Cauchy model in the 400–1700 nm range.

The surface morphology of the synthesized materials was studied using a field emission Zeiss Supra 25 scanning electron microscopy (SEM), operating at 3 kV. Prior to imaging, the samples were coated with a 3 nm-thick gold film using sputter deposition. The coating rendered the surfaces conductive, thus preventing electron beam charging of the insulating polymer.

The structure of the samples was investigated using a Bruker D-500

X-ray diffractometer (XRD), with a parallel Cu-Kα radiation, operating at 40 kV and 40 mA, over a 2θ range of 20°–60°, and grazing incidence mode (0.8°). The XRD patterns are reported in counts per second (cps) versus 2θ, and they were analyzed by the Bruker software suite, including the ICSD structure database.

In order to test a possible application of the materials synthetized, the photoactivity of the samples towards the degradation of methylene blue (MB) dye and sodium lauryl sulfate (SDS) was tested. The measurements were performed under UV light irradiation generated using a UWAVE led UV lamp system with an emission centered at 365 nm (full width at half maximum of 10 nm), and an irradiance of 12 mW/cm^2. Before taking any measurements, the samples were irradiated by the UV lamp for 60 min in order to remove the hydrocarbons from the surface of the specimens [41]. The samples were thereafter immersed in a 4 mL solution containing deionized water and an initial MB or SDS concentration of 1.5×10^{-5} M. Before switching on the UV light, the solutions were held in the dark for 1 h in order to assess the adsorption of the MB/SDS on the beaker surface and on the sample surface. The MB solution was then irradiated and measured at regular time intervals for up to 4 h, using a UV–vis spectrophotometer (Lambda 35, PerkinElmer) in a wavelength range of 500–800 nm. The degradation of MB was determined by measuring the absorbance of the 664 nm peak in the Lambert-Beer regime [42]. SDS degradation was tested after 4 h of UV irradiation using a visible spectrophotometer (Hach DR 3900), LCK 432 cuvette kits for high concentration solutions and LCK 332 cuvette kits for low concentration solutions. The experimental error of the photocatalytic measurements was 1%.

3. Results and discussion

ZnO thin films were deposited using ALD at a deposition temperature of 80 °C, with different cycles, i.e. thickness. Table 1 reports the values of the thicknesses of several ZnO layers deposited on Si or PMMA substrates for different ALD cycles. The values clearly indicate that with equal cycles the thicknesses obtained on the PMMA plates are lower than those on Si. This is due to the lack of reactive hydroxyl groups on the PMMA substrates, which hinders the atomic layer deposition, as discussed in detail in the introduction.

The growth rate of the ZnO thin films deposited on Si substrates was linearly extrapolated by the trend of the thickness versus the number of the cycles (Fig. 1). The growth rate for ZnO deposited on Si at 80 °C was 0.095 nm/cycle in agreement with the value extrapolated in our previous work [43]. As explained in the introduction to this work, the deposition of ZnO on PMMA substrates is more challenging and the infiltration of the precursors inside the porous polymeric matrix is required before onset of film growth. In fact, as evident from Fig. 1, over 550 cycles are required before a coating with a measurable thickness can be produced. After a 550-cycle barrier, the thickness of the ZnO film increases at a rate of 0.11 nm/cycle (being the linear fit performed for data with cycles higher than 550). This means that after a latency period (during which the diffusion and trapping of the precursors into the near surface region of the polymer take place), the growth rate of films deposited on PMMA is slightly higher than that on Si substrates, confirming the data already reported in the literature for other inorganic and organic materials [25,34].

Table 1
Thickness of ZnO thin films deposited using ALD on Si and PMMA substrates as a function of the deposition cycles.

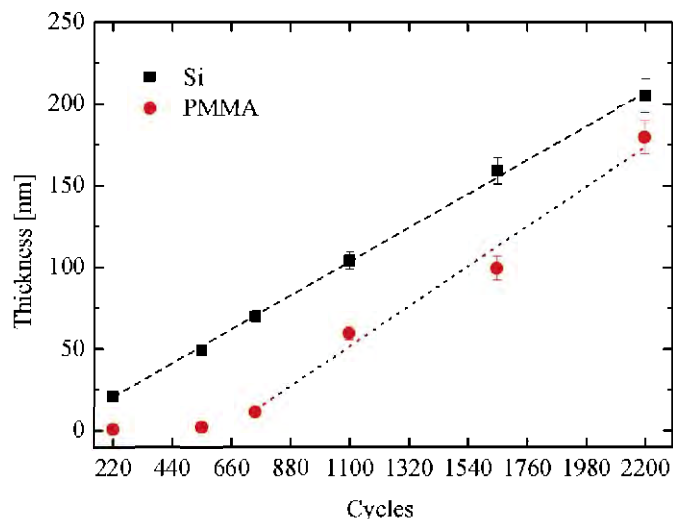| Cycles	ZnO thickness on Si (nm)	ZnO thickness on PMMA (nm)
220	21 ± 1	1 ± 0.1
550	49 ± 3	2.4 ± 0.1
750	70 ± 4	12 ± 2
1100	104 ± 5	60 ± 4
1650	159 ± 8	100 ± 7
2200	205 ± 10	180 ± 10

Fig. 1. Film thickness of ZnO deposited using ALD at 80 °C on Si (square) and on PMMA (circles) as a function of the number of the ALD cycles. Film growth rates were based on the linear fit of the experimental data (dashed lines).

The results reported from here on concern ZnO films deposited on PMMA substrates using ALD for a total of 1650 cycles, equivalent to a coating thickness of about 100 nm. The ZnO overlay deposited on PMMA powders had a thickness of approximately 80 nm, as measured by cross-sectional scanning electron microscope [16].

Fig. 2 shows plan-view scanning electron micrographs of the samples investigated. The morphology of the ZnO film deposited directly on PMMA samples, i.e. "ZnO ALD" is represented in Fig. 2 (a) where a ZnO film totally covers the PMMA substrates. The surface of the ZnO layer appears composed of small grains. The literature is indeed unanimous in reporting SEM images of ALD ZnO films with a granular structure [35, 43,44]. The high roughness of the film can be attributed to that of the polymeric substrate. Fig. 2 (b) shows the surface morphology of a "ZnO ALD + Solution Casting" sample. The specimen exhibits the granular structure of ZnO, deposited by ALD and then desegregated by the solution casting process. In this case, the presence of voids appears from the SEM analyses. Fig. 2 (c) demonstrates a plan-view SEM image of a "ZnO Solution Casting" sample, used as comparison for the present work. The figure clearly shows a PMMA matrix with several holes in which the ZnO embedded itself. The ZnO nanopowders, in the form of flakes, have the usual granular morphology [16,35].

XRD results reported in Fig. 3 clearly show that all the nanocomposites have the Wurtzite polycrystalline structure, typical for polycrystalline ZnO. In particular, the diffraction patterns reported in Fig. 3 have Bragg peaks corresponding to the planes (100), (002), (101), and (110) at 31.85°, 34.35°, 36.25°, 44.75°, 56.75° in agreement with the Joint Committee on Powder Diffraction Standards (JCPDS) card of ZnO [JCPDS 36–1451]. Therefore, despite the low fabrication temperature (80 °C in the case of the ALD process and room temperature in the case of solution casting) all the samples exhibited a high degree of crystallinity. It is important to note that a broad band is observed in all coatings except the "ZnO ALD" films. The broad band is the result of the PMMA amorphous structure. The sharper "ZnO ALD" peaks can be attributed to the higher ZnO film thickness that isolated the polymeric substrate.

In order to give a proof of concept of the feasibility of the nanocomposites synthesized in this work, the photocatalytic activity of the materials in the degradation of two organic pollutants was tested: methylene blue dye and sodium lauryl sulfate. The amount of ZnO in all the specimens was indirectly estimated with the aim to compare the synthesized samples correctly and to use the same amount of ZnO for all the experiments. For the "ZnO ALD" material, a sample with an area of 2
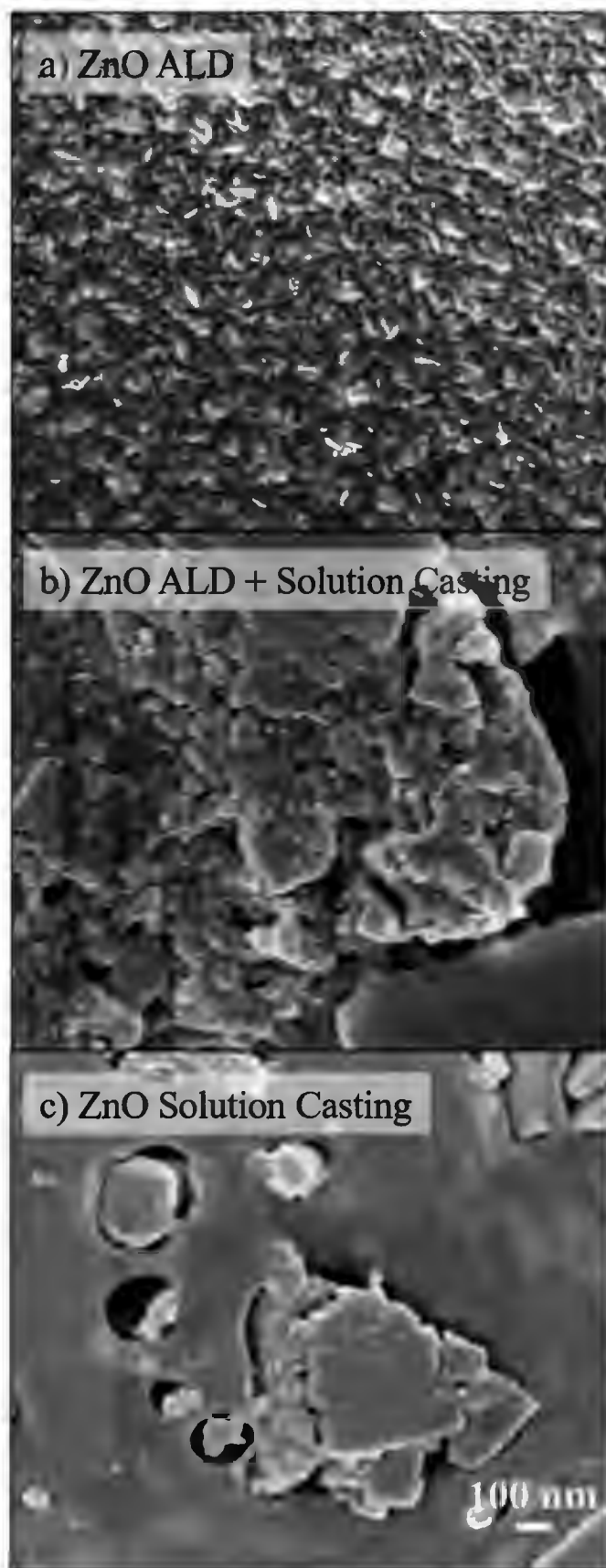
Fig. 2. Plan-view SEM images of ZnO-PMMA composites: a) "ZnO ALD", b) "ZnO ALD + Solution Casting", and c) "ZnO Solution Casting" samples.
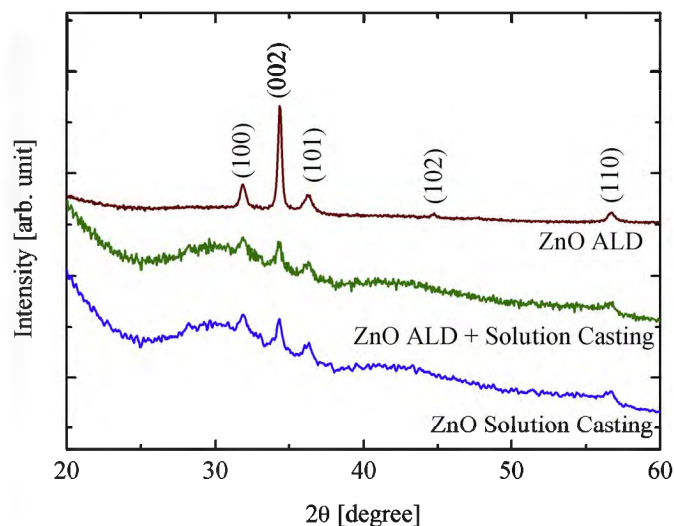

Fig. 3. XRD patterns of ZnO-PMMA composites (from the top to the bottom): "ZnO ALD", "ZnO ALD + Solution Casting", and "ZnO Solution Casting".

cm^2 was calcined at 800 °C in air for 3 h to remove all the PMMA used as substrate. The amount of ZnO powder after the calcination was 0.3 mg resulting in a concentration of 0.15 mg/cm². The "ZnO ALD + Solution Casting" sample had approximately 2% ZnO, as determined by the variation of the weight before and after the deposition [16]. The amount of coated PMMA was 300 mg, meaning 6 mg of ZnO in a Petri dish with a diameter of 5 cm, giving a concentration of ZnO of 0.30 mg/cm². Lastly, for the "ZnO Solution Casting" samples, 30 mg of ZnO powders were mixed with 300 mg of PMMA so the concentration of ZnO in a Petri dish with a diameter of 5 cm was 1.5 mg/cm². The size of each squared samples was consequently selected to provide the same amount of ZnO for each sample typology. The sample sizes were consequently set at 2.5 × 2.5 cm², 1,8 × 1,8 cm², and 0.8 × 0.8 cm² for the "ZnO ALD", "ZnO ALD + Solution Casting", and "ZnO Solution Casting" sample, respectively.

The photocatalytic activity of these samples was firstly evaluated by the degradation of MB under UV light irradiation. The experimental results were reported in Fig. 4. In the figure, C indicates the concentration of MB at time t, and C_0 is the starting concentration of MB. The discoloration of the aqueous solutions was tested in the absence of any
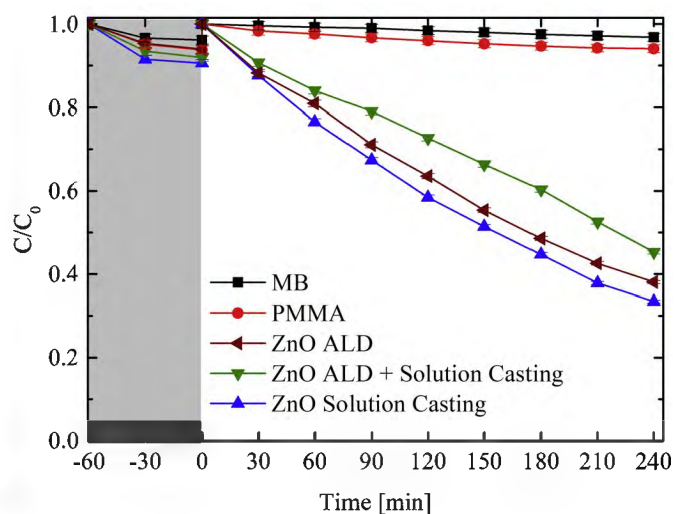

Fig. 4. MB photodegradation under UV light irradiation for five samples: MB (squares), bare PMMA (circles), MB with "ZnO ALD" (left triangles), "ZnO ALD + Solution Casting" (down triangles), "ZnO Solution Casting" (up triangles).

photocatalytic materials (squares) and in the presence of bare PMMA plates (circles) as controls, and also with the synthesized nanocomposites: "ZnO ALD" (left triangles), "ZnO ALD + Solution casting" (down triangles), and "ZnO Solution Casting" (up triangles). The adsorption capacity of the samples was preliminarily tested in the dark until equilibrium was reached (grey area in Fig. 4). This step was important to discern the photocatalysis of the materials from the adsorbance of the dye to the beaker walls and/or sample surfaces. After 1 h in the dark, a slight adsorption of MB can be observed with all samples, following which equilibrium is reached. Afterwards, the UV light is turned on. As expected, no response was obtained in the two MB solutions without any catalysts (i.e. MB aqueous solution, MB with virgin PMMA). On the other hand, MB solutions with ZnO-enriched samples showed significant discoloration. The "ZnO ALD" samples were able to degrade ~ 62% of the starting concentration of MB, the "ZnO ALD + Solution Casting" samples were able to degrade ~ 55%, and the "ZnO Solution Casting" samples removed ~ 67%. The slight differences in the efficiency could be due to the errors in the indirect evaluation of the amount of ZnO in the different samples and to a diverse nanostructure of the specimens. In any case, all samples exhibited considerable efficacy in the degradation of MB dye.

The photocatalytic activity of the synthesized materials was assessed for the degradation of sodium lauryl sulfate, an anionic surfactant frequently used in many cleaning and hygiene products for its foaming effect. The results are reported in Fig. 5, where the percentage of the SDS degradation is measured after 4 h of UV light exposure. The results indicate that all samples can efficiently degrade the surfactant. The degradation percentage is higher than in the case of MB: ~ 64% for the "ZnO ALD", ~ 66% for the "ZnO ALD + Solution Casting", and ~ 73% for the "ZnO Solution Casting" samples. This is probably due to the difference in charge between the SDS and the MB. In fact, the partial positive charge of the ZnO [45] favors the interaction between the semiconductor surface and the anionic surfactant, but hinders the interaction with the MB, that is positively charged.

4. Conclusions

In summary, the synthesis of hybrid systems consisting of ZnO and PMMA was reported. Three different strategies for the production of ZnO-PMMA nanocomposites were reported, namely: 1) the deposition of ZnO thin films by ALD on PMMA plates; 2) the covering of PMMA powders by thin layers of ZnO using ALD and the subsequent formation of specimens by sonication and solution casting; 3) the sonication and solution casting of ZnO nanopowders and PMMA. It was found that the ALD of ZnO on PMMA plates at low temperature suffers from a latency period (during which the diffusion and trapping of the precursors into the near surface region of the polymer take place); afterwards, the growth of the ZnO films deposited on PMMA proceeds more quickly than that on Si substrates. XRD analyses proved the polycrystalline structure of the ZnO in all the sample typologies, despite the low fabrication temperature (80 °C in case of the ALD process and room temperature in case of the solution casting one). The high photocatalytic activity of the nanocomposites was verified using the degradation of methylene blue and sodium lauryl sulfate (a dye and an anionic surfactant, respectively) in water by UV light irradiation. The results reported here show that ZnO-PMMA nanocomposites can be easily synthetized and used in wastewater treatment, but also in devices such as sensors, photovoltaics and optoelectronics.

Declaration of competing interest

The authors declare that they have no known competing financial interests or personal relationships that could have appeared to influence the work reported in this paper.
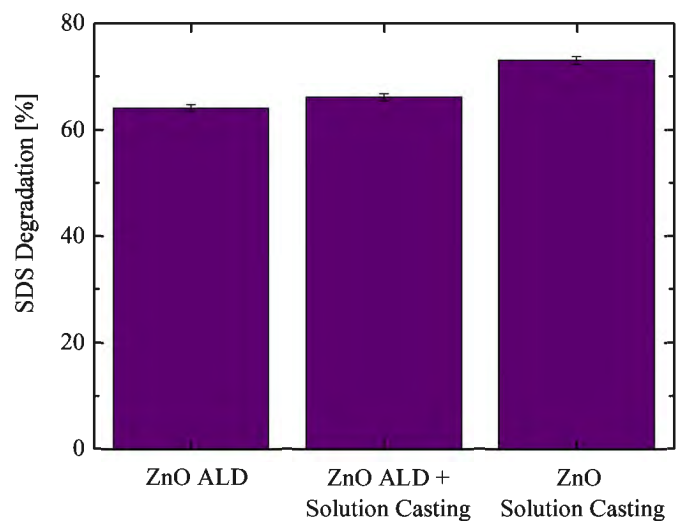

Fig. 5. SDS photodegradation under UV light radiation for the investigated samples: "ZnO ALD", "ZnO ALD + Solution Casting", and "ZnO Solution Casting".

Acknowledgements

References

[1] Ü. Özgür, Ya I. Alivov, C. Liu, A. Teke, M.A. Reshchikov, S. Doğan, V. Avrutin, S.-J. Cho, H. Morkoç, A comprehensive review of ZnO materials and devices, J. Appl. Phys. 98 (2005), https://doi.org/10.1063/1.1992666, 041301 (103 pp).

[2] I. Udom, M.K. Ram, E.K. Stefanakos, A.F. Hepp, D.Y. Goswami, One dimensional-ZnO nanostructures: synthesis, properties and environmental applications, Mater. Sci. Semicond. Process. 16 (2013) 2070–2083, https://doi.org/10.1016/j.mssp.2013.06.017.

[3] Y.K. Mishra, R. Adelung, ZnO tetrapod materials for functional applications, Mater. Today 21 (2018) 631–651, https://doi.org/10.1016/j.mattod.2017.11.003.

[4] J. Theerthagiri, S. Salla, R.A. Senthil, P. Nithyadharseni, A. Madankumar, P. Arunachalam, T. Maiyalagan, H.-S. Kim, A review on ZnO nanostructured materials: energy, environmental and biological applications, Nanotechnology 30 (2019), https://doi.org/10.1088/1361-6528/ab268a, 392001 (27 pp).

[5] K.M. Lee, C.W. Lai, K.S. Ngai, J.C. Juan, Recent developments of zinc oxide based photocatalyst in water treatment technology: a review, Water Res. 88 (2016) 428–448, https://doi.org/10.1016/j.watres.2015.09.045.

[6] S.G. Kumar, K.S.R.K. Rao, Zinc oxide based photocatalysis: tailoring surface-bulk structure and related interfacial charge carrier dynamics for better environmental applications, RSC Adv. 5 (2015) 3306–3351, https://doi.org/10.1039/C4RA13299H.

[7] A. Di Mauro, M. Zimbone, M. Scuderi, G. Nicotra, M.E. Fragalà, G. Impellizzeri, Effect of Pt nanoparticles on the photocatalytic activity of ZnO nanofibers, Nanoscale Res. Lett. 10 484 (2015) 1–7, https://doi.org/10.1186/s11671-015-1126-6.

[8] M. Cantarella, A. Di Mauro, A. Gulino, L. Spitaleri, G. Nicotra, V. Privitera, G. Impellizzeri, Selective photodegradation of paracetamol by molecularly imprinted ZnO nanonuts, Appl. Catal. B Environ. 238 (2018) 509–517, https://doi.org/10.1016/j.apcatb.2018.07.055.

[9] Z.L. Wang, Nanostructures of zinc oxide, Mater. Today 7 (2004) 26–33.

[10] Q. Li, V. Kumar, Y. Li, H. Zhang, T.J. Marks, R.P.H. Chang, Fabrication of ZnO nanorods and nanotubes in aqueous solutions, Chem. Mater. 17 (2005) 1001–1006, https://doi.org/10.1021/cm048144q.

[11] S. Baruah, J. Dutta, Hydrothermal growth of ZnO nanostructures, Sci. Technol. Adv. Mater. 10 (2009), https://doi.org/10.1088/1468-6996/10/1/013001, 013001 (18 pp).

[12] A. Di Mauro, M. Zimbone, M. Scuderi, G. Nicotra, M.E. Fragalà, G. Impellizzeri, Synthesis of ZnO nanofibers by the electrospinning process, Mater. Sci. Semicond. Process. 42 (2016) 98–101, https://doi.org/10.1016/j.mssp.2015.08.003.

[13] A. Di Mauro, M.E. Fragalà, V. Privitera, G. Impellizzeri, ZnO for application in photocatalysis: from thin films to nanostructures, Mater. Sci. Semicond. Process. 69 (2017) 44–51, https://doi.org/10.1016/j.mssp.2017.03.029.

[14] A. Nicolay, A. Lanzutti, M. Poelman, B. Ruelle, L. Fedrizzi, Ph Dubois, M.-G. Oliver, Elaboration and characterization of a multifunctional silane/ZnO hybrid nanocomposite coating, Appl. Surf. Sci. 327 (2015) 379–388, https://doi.org/10.1016/j.apsusc.2014.11.161.

[15] V.E. Podasca, T. Buruiana, E.C. Buruiana, UV-cured polymeric films containing ZnO and silver nanoparticles with UV-vis light-assisted photocatalytic activity,

Appl. Surf. Sci. 377 (2016) 262–273, https://doi.org/10.1016/j.apsusc.2016.03.178.

[16] A. Di Mauro, M. Cantarella, G. Nicotra, G. Pellegrino, A. Gulino, M.V. Brundo, V. Privitera, G. Impellizzeri, Novel synthesis of ZnO/PMMA nanocomposites for photocatalytic applications, Sci. Rep. 7 (12pp) (2017) 40895, https://doi.org/10.1038/srep40895.

[17] G. Pellegrino, S.C. Carroccio, F. Ruffino, G.G. Condorelli, G. Nicotra, V. Privitera, G. Impellizzeri, Polimeric platform for the growth of chemically anchored ZnO nanostructures by ALD, RSC Adv. 8 (2018) 521–530, https://doi.org/10.1039/c7ra11168a.

[18] M. Ussia, A. Di Mauro, T. Mecca, F. Cunsolo, G. Nicotra, C. Spinella, P. Cerruti, G. Impellizzeri, V. Privitera, S.C. Carroccio, ZnO-pHEMA nanocomposites: an ecofriendly and reusable material for water remediation, ACS Appl. Mater. Interfaces 10 (2018) 40100–40110, https://doi.org/10.1021/acsami.8b13029.

[19] D. Ponnammaa, J.-J. Cabibihan, M. Rajan, S.S. Pethaiah, K. Deshmukh, J.P. Gogoi, S.K.K. Pasha, M.B. Ahamed, J. Krishnegowda, B.N. Chandrashekar, A.R. Polu, C. Cheng, Synthesis, optimization and applications of ZnO/polymer nanocomposites, Mater. Sci. Eng. C 98 (2019) 1210–1240, https://doi.org/10.1016/j.msec.2019.01.081.

[20] M. Abbas, M. Buntinx, W. Deferme, R. Peeters, (Bio)polymer/ZnO nanocomposites for packaging applications: a review of gas barrier and mechanical properties, Nanomaterials 9 (14 pp) (2019) 1494, https://doi.org/10.3390/nano9101494.

[21] D. Barreca, E. Comini, A.P. Ferrucci, A. Gasparotto, C. Maccato, C. Maragno, G. Sberveglieri, E. Tondello, First example of ZnO-TiO$_2$ nanocomposites by chemical vapor deposition: structure, morphology, composition, and gas sensing performances, Chem. Mater. 19 (2007) 5642–5649, https://doi.org/10.1021/cm701990f.

[22] W. Yang, J. Liu, Z. Guan, Z. Liu, B. Chen, L. Zhao, Y. Li, X. Cao, X. He, C. Zhang, Q. Zeng, Y. Fu, Morphology, electrical and optical properties of magnetron sputtered porous ZnO thin films on Si(100) and Si(111) substrates, Ceram. Int. 46 (2020) 6605–6611, https://doi.org/10.1016/j.ceramint.2019.11.147.

[23] N. Pinna, M. Knez (Eds.), Atomic Layer Deposition of Nanostructured Materials, Wiley-VCH, Weinheim, Germany, 2012.

[24] S.M. George, Atomic layer deposition: an overview, Chem. Rev. 110 (2010) 111–131, https://doi.org/10.1021/cr900056b.

[25] H.C. Guo, E. Ye, Z. Li, M.-Y. Han, X.J. Loh, Recent progress of atomic layer deposition on polymeric materials, Mater. Sci. Eng. C 70 (2017) 1182–1191, https://doi.org/10.1016/j.msec.2016.01.093.

[26] J.S. King, E. Graugnard, O.M. Roche, D.N. Sharp, J. Scrimgeour, R.G. Denning, A. J. Turberfield, C.J. Summers, Infiltration and inversion of holographically defined polymer photonic crystal templates by atomic layer deposition, Adv. Mater. 18 (2006) 1561–1565, https://doi.org/10.1002/adma.200502287.

[27] X. Liang, L.F. Hakim, G.-D. Zhan, J.A. McCormick, S.M. George, A.W. Weimer, Novel processing to produce polymer/ceramic nanocomposites by atomic layer deposition, J. Am. Ceram. Soc. 90 (1) (2007) 57–63, https://doi.org/10.1111/j.1551-2916.2006.01359.x.

[28] Q. Peng, Y.-C. Tseng, S.B. Darling, J.W.E.Q. Peng, Y.-C. Tseng, S.B. Darling, J. W. Elam, Nanoscopic patterned materials with tunable dimensions via atomic layer deposition on block copolymers, Adv. Mater. 22 (2010) 5129–5133, https://doi.org/10.1002/adma.201002465.

[29] J. Kamcev, D.S. Germack, D. Nykypanchuk, R.B. Grubbs, C.-Y. Nam, C.T. Black, Chemically enhancing block copolymers for block-selective synthesis of self-assembled metal oxide nanostructures, ACS Nano 7 1 (2013) 339–346, https://doi.org/10.1021/nn304122b.

[30] N. Li, J. Zhang, Y. Tian, J. Zhang, W. Zhan, J. Zhao, Y. Ding, W. Zuo, Hydrophilicmodification of polyvinylidene fluoride membranes by ZnO atomic layer deposition using nitrogen dioxide/diethylzinc functionalization, J. Membr. Sci. 514 (2016) 241–249, https://doi.org/10.1016/j.memsci.2016.04.072.

[31] T. Tynell, M. Karppinen, ZnO: hydroquinone superlattice structures fabricated by atomic/molecular layer deposition, Thin Solid Films 551 (2014) 23–26, https://doi.org/10.1016/j.tsf.2013.11.067.

[32] M. Vähä-Nissi, M. Pitkänen, E. Salo, E. Kenttä, A. Tanskanen, T. Sajavaara, M. Putkonen, J. Sievänen, A. Sneck, M. Rättö, M. Karppinen, A. Harlin, Antibacterial and barrier properties of oriented polymer films with ZnO thin films applied with atomic layer deposition at low temperatures, Thin Solid Films 562 (2014) 331–337, https://doi.org/10.1016/j.tsf.2014.03.068.

[33] L.E. Ocola, A. Connolly, D.J. Gosztola, R.D. Schaller, A. Yanguas-Gil, Infiltrated zinc oxide in poly(methyl methacrylate): an atomic cycle growth study, J. Phys. Chem. C 121 (2017) 1893–1903, https://doi.org/10.1021/acs.jpcc.6b08007.

[34] C.A. Wilson, R.K. Grubbs, S.M. George, Nucleation and growth during Al$_2$O$_3$ atomic layer deposition on polymers, Chem. Mater. 17 (2005) 5625–5634, https://doi.org/10.1021/cm050704d.

[35] M. Napari, J. Malm, R. Lehto, J. Julin, K. Arstila, T. Sajavaara, M. Lahtinen, Nucleation and growth of ZnO on PMMA by low-temperature atomic layer deposition, J. Vac. Sci. Technol., A 33 (2015), https://doi.org/10.1116/1.4902326, 01A128 (7 pp).

[36] A. Singh, A. Mathur, D. Pal, A. Sengupta, R. Singh, S. Chattopadhyay, Near room temperature atomic layer deposition of ZnO thin films on poly (methyl methacrylate) (PMMA) templates: a study of structure, morphology and photoluminescence of ZnO as an effect of template confinement, Vacuum 161 (2019) 398–403, https://doi.org/10.1016/j.vacuum.2019.01.006.

[37] B.J. Ash, L. S Schadler, R. W Siegel, Glass transition behavior of alumina/polymethylmethacrylate nanocomposites, Mater. Lett. 55 (1–2) (2002) 83–87, https://doi.org/10.1016/S0167-577X(01)00626-7.

[38] K. Oksman, et al. (Eds.), Handbook of Green Materials: Processing Technologies, Properties and Applications, vol. 5, World Scientific, 2014 (chapter 4).

[39] M. Cantarella, R. Sanz, M.A. Buccheri, F. Ruffino, G. Rappazzo, S. Scalese, G. Impellizzeri, L. Romano, V. Privitera, Immobilization of nanomaterials in PMMA composites for photocatalytic removal of dyes, phenols and bacteria from water, J. Photochem. Photobiol. Chem. 321 (2016) 1–11, https://doi.org/10.1016/j.jphotochem.2016.01.020.

[40] A. Sadollahkhani, I. Kazeminezhad, J. Lu, O. Nur, L. Hultman, M. Willander, Synthesis, structural characterization and photocatalytic application of ZnO@ZnS core-shell nanoparticles, RSC Adv. 4 (2014) 36940–36950, https://doi.org/10.1039/C4RA05247A.

[41] R. Wang, K. Hashimoto, A. Fujishima, M. Chikuni, E. Kojima, A. Kitamura, M. Shimohigoshi, T. Watanabe, Light-induced amphiphilic surfaces, Nature 388 (1997) 431–432, https://doi.org/10.1038/41233.

[42] Compendium of chemical terminology, in: A.D. McNaught, A. Wilkinson (Eds.), The Gold Book, second ed., Blackwell Scientific Publications, Oxford, 1997.

[43] A. Di Mauro, M. Cantarella, G. Nicotra, V. Privitera, G. Impellizzeri, Low temperature atomic layer deposition of ZnO: applications in photocatalysis, Appl. Catal. B Environ. 196 (2016) 68–76, https://doi.org/10.1016/j.apcatb.2016.05.015.

[44] E. Guziewicz, I.A. Kowalik, M. Godlewski, K. Kopalko, V. Osinniy, A. Wójcik, S. Yatsunenko, E. Łusakowska, W. Paszkowicz, M. Guziewicz, Extremely low temperature growth of ZnO by atomic layer depoisition, J. Appl. Phys. 103 (2008), https://doi.org/10.1063/1.2836819, 033515 1-6.

[45] M. Giahia, S. Habibib, S. Totonchib, M. Khavei, Photocatalytic degradation of anionic surfactant using zinc oxide nanoparticles, Russ. J. Phys. Chem. A 86 4 (2012) 689–693, https://doi.org/10.1134/S0036024412040103.